Check for updates

European Journal of Immunology

WILEY-VCH

European Journal of Immunology
Basic • Clinical • Translational

TECHNICAL REPORT OPEN ACCESS

Multi-Parameter Spectral Flow Cytometry Panel for Immune Phenotyping of Murine B and T Cell Responses

Kassandra Hoetzel[1,2] | Hendrik Feuerstein[1,2] | Julia Ludwig[1] | Hedda Wardemann[1]

[1]B Cell Immunology, German Cancer Research Center (DKFZ), Heidelberg, Germany | [2]Faculty of Biosciences, Heidelberg University, Heidelberg, Germany

Correspondence: Hedda Wardemann (h.wardemann@dkfz-heidelberg.de)

Received: 18 July 2025 | **Revised:** 20 March 2026 | **Accepted:** 23 March 2026

Keywords: B cells | spectral flow cytometry | T cells | vaccination

The primary site of T cell-dependent B cell immune responses are the germinal centers (GCs) within secondary lymphoid organs [1]. In these microanatomical structures, antigen-activated B cells undergo affinity maturation, a process in which somatically mutated B cells with improved antigen-binding capacity are selected through competition for antigen and T cell help, before differentiating into antibody-secreting cells and memory B cells [1, 2]. While the majority of newly generated antibody-secreting cells are short-lived plasmablasts (PB), a subset can home to dedicated survival niches in the bone marrow and differentiate into long-lived plasma cells (PCs), thereby mediating durable humoral immunity. During recall responses, memory B cells rapidly develop into antibody-secreting cells, contributing to the swift production of antigen-specific serum antibodies.

Here, we describe a 31-parameter spectral flow panel for the deep phenotypic analysis of antigen-specific B cell responses [3–14]. The panel was established using a full visible spectrum cytometer (BD FACSymphony A5 SE Cell Analyzer) equipped with 5 lasers and 49 detectors (Tables S1 and S2, Figure S1) and lymph node, spleen, and bone marrow samples from non-immunized mice and mice immunized with trimeric SARS-CoV-2 prefusion spike protein stabilized by six prolines (S6P). Antigen-reactive B cells were identified using fluorochrome-labeled S6P and SARS-CoV-2 receptor-binding domain (RBD) baits. The materials and methods, including the antibody list (Table S3), single-color reference controls and N × N plots (Table S4, Figure S2), the antibody titration process (Figure S3), and antigen bait staining (Figures S4 and S5) as well as limitations of the study are described in the Supporting Information. Moreover, a summary of the panel design and optimization process is provided in Tables S5 and S6.

Regardless of the tissue of origin, single lymphocytes from all organs were identified based on their size and granularity (Figures 1A and 2A). Next, dead cells, as well as natural killer cells, erythrocytes, monocytes (including neutrophils), macrophages, and dendritic cells (collectively referred to as lineage-negative [Lin$^-$] cells), were excluded from the analysis. This was achieved using a fixable viability stain (440UV) and a lineage antibody mix (anti-NK-1.1, anti-TER-119, anti-Ly-6G/Ly-6C [Gr-1], anti-F4/80, and anti-CD11c), all conjugated to the same fluorochrome [3]. Then, sequential gating was applied to identify each B and T cell subset unambiguously.

Immunization led to the development of PCs, which were identified by the expression of CD138 and the transmembrane activator and CAML interactor (TACI) (Figures 1B and 2B, Figures S6, S9, S10, and S11) [11–13]. Three PC subsets (P1-3) were discriminated based on their CD19 and B220 expression: P1- PC precursors (B220^{int}CD19^{int}), P2-early PCs (B220^{low}CD19^{int}), and P3-mature PCs (B220^{low}CD19^{low}). The panel includes markers tailored for the analysis of long-lived PCs [12] including antibodies against TIGIT, which is predominantly expressed on PC precursors (P1) and early PCs (P2), as well as CXCR3, Ep-CAM, and Ly6A, markers associated with IgG (Ep-CAM$^+$CXCR3$^-$) or IgA (Ly6A$^+$TIGIT$^-$) expression [12, 13].

Abbreviations: CM, Central memory; EM, Effector memory; FO, Follicular; GC, Germinal center; MZ, Marginal zone; PaCMAP, Pairwise controlled manifold approximation and projection; PB, Plasmablast; PC, Plasma cell; RBD, SARS-CoV-2 receptor-binding domain; S6P, SARS-CoV-2 prefusion spike protein stabilized by six prolines; TACI, Transmembrane activator and CAML interactor; Tfh, T follicular helper (cell).

This is an open access article under the terms of the Creative Commons Attribution License, which permits use, distribution and reproduction in any medium, provided the original work is properly cited.

© 2026 The Author(s). *European Journal of Immunology* published by Wiley-VCH GmbH.

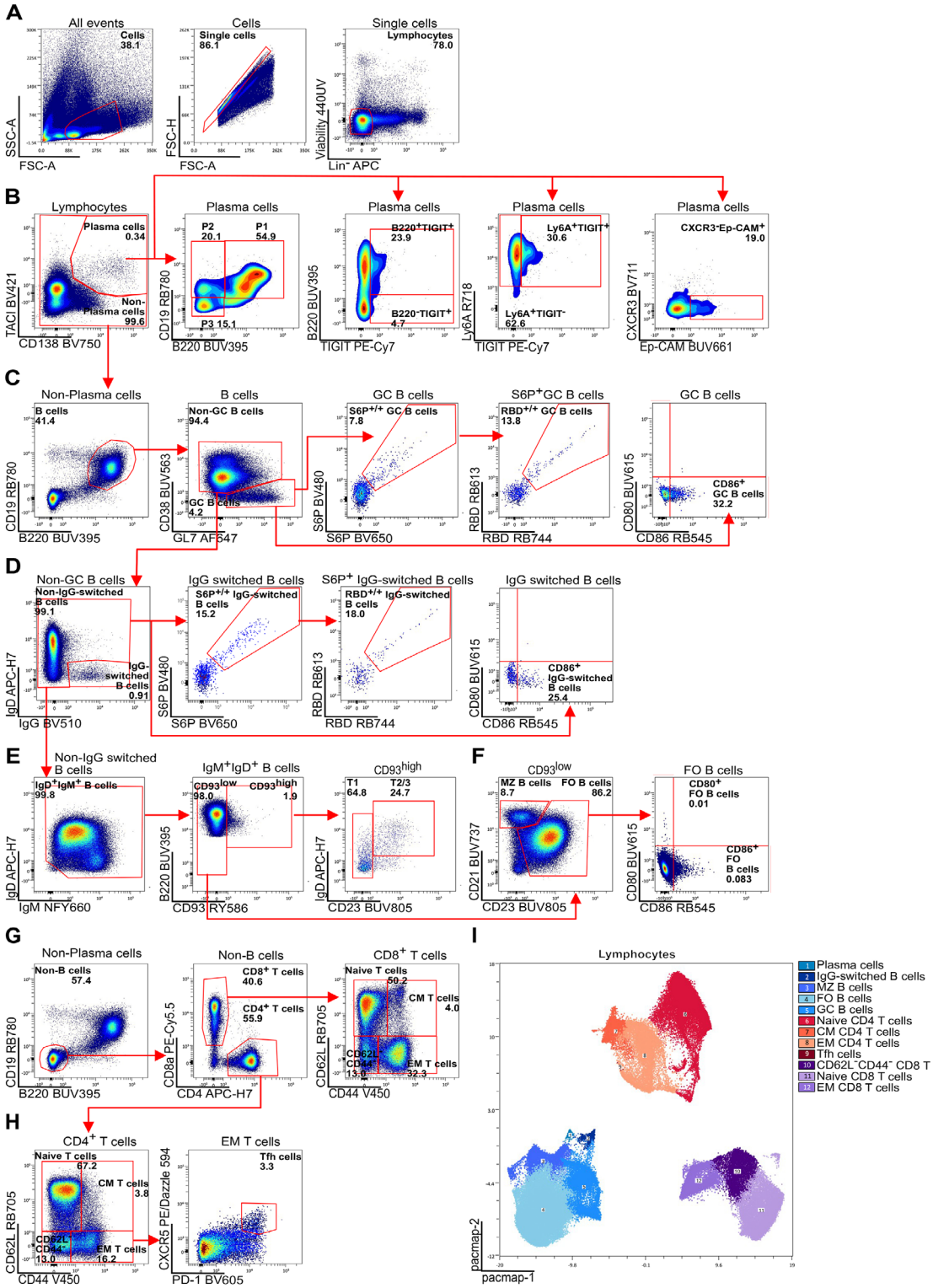


FIGURE 1 | Gating strategy for murine spleen samples from an immunized mouse. (A) Viable lymphocytes. (B) PCs ($TACI^{int}CD138^{+}$) were further subdivided into three subsets: P1 ($B220^{int}CD19^{int}$), P2 ($B220^{low}CD19^{int}$), and P3 ($B220^{low}CD19^{low}$). PCs with Ep-$CAM^{high}CXCR3^{-}$ or $Ly6A^{high}TIGIT^{-}$ phenotypes were identified. (C) GC B cells ($CD38^{-}GL7^{+}$) were investigated for antigen reactivity ($S6P^{+/+}$, $RBD^{+/+}$) and activation status ($CD86^{+}$). (D) IgG^{+} class-switched B cells ($CD38^{+}GL7^{-}IgG^{+}$) showed antigen-reactivity ($S6P^{+/+}$, $RBD^{+/+}$) and expressed the activation marker CD86. (E) $B220^{+}CD93^{high}$ T1- ($IgM^{high}CD23^{low}$) and T2-stage ($IgD^{high}CD23^{high}$) transitional B cells were identified. (F) $B220^{+}CD93^{low}$ naive follicular ($CD23^{high}CD21^{+}$) and marginal zone ($CD23^{low}CD21^{high}$) B cells were defined. Activated naive follicular B cells ($CD80^{+}$ or $CD86^{+}$) were characterized. (G) Among $CD8^{+}$ T cells, naive ($CD44^{-}CD62L^{+}$), CM ($CD44^{+}CD62L^{+}$), and EM ($CD44^{+}CD62L^{-}$) were distinguished. (H) Similarly, naive, CM, and EM $CD4^{+}$ T cells were distinguished. EM $CD4^{+}$ T cells were further gated to identify Tfh cells ($CXCR5^{+}PD\text{-}1^{+}$). (I) PaCMAP (2D; kNN = 30, mid = 0.5, far = 2600 iters, Euclidean, random init) with FlowSOM metaclusters ($k = 16$) overlaid to show B/T-cell phenotypic heterogeneity. Data shown are representative of three mice ($n = 3$) from one experiment.

15214141, 2026, 4, Downloaded from https://onlinelibrary.wiley.com/doi/10.1002/eji.70182 by Dagmar Stiek - Deutsches Krebsforschungszentrum (DKFZ) , Wiley Online Library on [09/06/2026]. See the Terms and Conditions (https://onlinelibrary.wiley.com/terms-and-conditions) on Wiley Online Library for rules of use; OA articles are governed by the applicable Creative Commons License

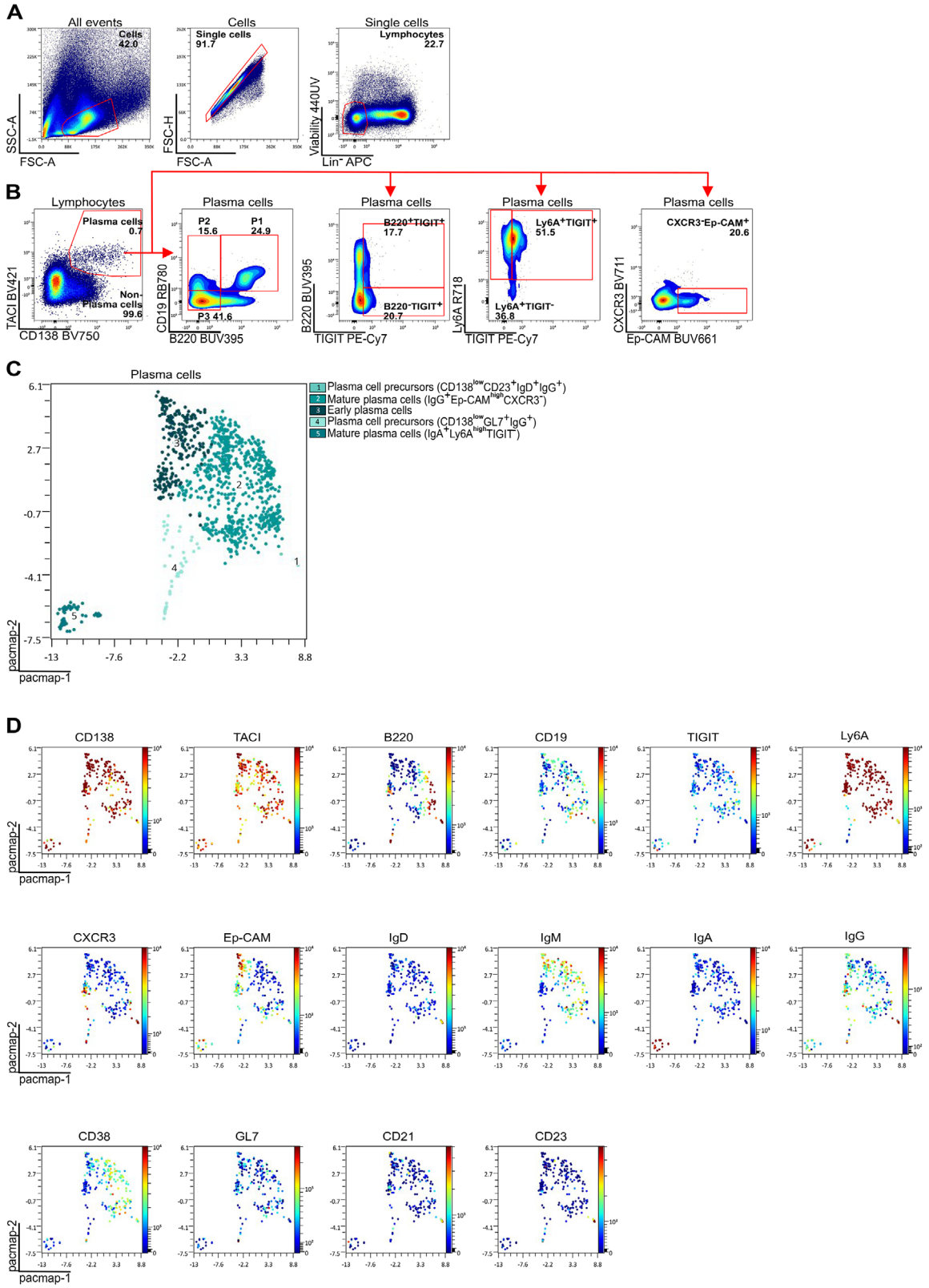


FIGURE 2 | Gating strategy for murine bone marrow PC subsets. (A) Viable lymphocytes. (B) PCs ($TACI^{int}CD138^{+}$) subsets: P1 ($B220^{int}CD19^{int}$), P2 ($B220^{low}CD19^{int}$), and P3 ($B220^{low}CD19^{low}$). PCs with Ep-$CAM^{+}CXCR3^{-}$ or $Ly6A^{+}TIGIT^{-}$ phenotypes were distinguished. (C) PaCMAP (2D; kNN = 30, mid = 0.5, far = 2600 iters, Euclidean, random init, seed = 4786) with FlowSOM metaclusters ($k = 5$) overlaid to show antibody-secreting cell differentiation diversity. (D) Selected marker expression is overlaid as a continuous color gradient on the PaCMAP to define PC subsets. Data shown are representative of three mice ($n = 3$) from one experiment.

15214141, 2026, 4, Downloaded from https://onlinelibrary.wiley.com/doi/10.1002/eji.70182 by Dagmar Stiek - Deutsches Krebsforschungszentrum (DKFZ) , Wiley Online Library on [09/06/2026]. See the Terms and Conditions (https://onlinelibrary.wiley.com/terms-and-conditions) on Wiley Online Library for rules of use; OA articles are governed by the applicable Creative Commons License

B cells were identified based on the lineage markers CD19 and B220. Among these, GC B cells were defined as $GL7^{+}CD38^{-}$. While GC B cells were rare in non-immunized mice, they were clearly detectable in the spleen and lymph nodes of immunized animals (Figure 1C and Figures S6, S9, and S10). These GC B cell populations included a substantial fraction of S6P and RBD bait-reactive cells, as well as $CD86^{high}$ cells, phenotypically resembling light zone GC B cells (Figure 1C) [1, 7–10].

In the spleen, CD38 was expressed on marginal zone (MZ), naive follicular (FO), transitional, and IgG^{+} class-switched B cells (Figure S7). To better separate the IgG^{+} class-switched B cells, isotype-specific antibodies were used (Figure S8). The frequency of IgG^{+} class-switched B cells was higher in immunized mice, including IgG^{+} cells that bound antigen (S6P, RBD) and expressed the activation marker CD86 reminiscent of memory B cells (Figure 1D and Figure S6). Antibodies against CD93, CD21, and CD23 enabled the discrimination of transitional B cell subsets (T1 – $CD93^{high}IgD^{neg/low}CD23^{-}$; T2/T3 – $CD93^{low}IgD^{low/pos}CD23^{+}$) from MZ ($IgM^{+}CD21^{high}CD23^{low}$) and naive FO ($IgD^{+}IgM^{int\text{-}low}CD23^{high}CD21^{+}$) B cells in spleen (Figure 1E,F) [4, 5, 8]. In immunized, but not in non-immunized, mice, naive FO B cells expressed higher levels of the activation marker CD80 but not CD86 (Figure 1F and Figure S6).

To facilitate the parallel assessment of T cell responses, antibodies against CD4 and CD8 were included in the panel (Figure 1G) [1, 8, 14, 15]. CD4 and CD8 T cells were further characterized based on the expression of CD44 and CD62L to distinguish naive ($CD44^{-}CD62L^{+}$), effector memory (EM; $CD44^{+}CD62L^{-}$), and central memory (CM; $CD44^{+}CD62L^{+}$) subsets (Figure 1G,H). CXCR5 and PD-1 expression on EM CD4 T cells was used to identify T follicular helper (Tfh) cells (Figure 1H). As CD62L is sensitive to enzymatic shedding, we caution that its detection may be impaired in thawed samples due to ex vivo processing, affecting the detection of naive and CM T cell subsets. To preserve reliable CD62L staining, we recommend using freshly prepared samples, minimizing incubation steps at room temperature, avoiding mechanical stress, and keeping samples on ice during processing whenever possible (Figure S12). Pairwise controlled manifold approximation and projection was used to distinguish the diverse cellular subsets (Figures 1I and 2C,D, Figure S13).

In summary, this 31-parameter spectral flow cytometry panel allows for the high-resolution phenotypic discrimination of diverse murine B and T cell subsets, with particular focus on antigen-experienced B cells, including rare subpopulations such as long-lived PCs and isotype-switched (memory) B cells. It is ideally suited for analyzing immunization or infection-induced immune responses in lymph nodes, spleen, and bone marrow.

Author Contributions

H.W. designed the study, interpreted data, and wrote the manuscript. K.H. designed the study, performed experiments, interpreted data, and wrote the manuscript. H.F. and J.L. performed experiments and interpreted data.

Acknowledgments

The authors thank the DKFZ Core Facility and BD Biosciences for technical support during panel optimization. We thank the Vaccine Formulation Institute for providing S6P formulated in adjuvant.

Open access funding enabled and organized by Projekt DEAL.

Funding

This work was supported by the Helmholtz Association's Initiative and Networking Fund project "Virological and immunological determinants of COVID-19 pathogenesis-lessons to get prepared for future pandemics (KA1-Co-02_CoViPa)." H.F. and K.H. were supported by the DKFZ International PhD Program.

Ethics Statement

All C57BL/6J mouse procedures were approved by the Regierungspräsidium Karlsruhe, Germany (Project Number: G27/23) and experiments were conducted in accordance with the German Animal Protection Law.

Conflicts of Interest

The authors declare no conflicts of interest.

Data Availability Statement

The flow cytometry files are available from the corresponding author upon request.

Peer Review

The peer review history for this article is available at https://publons.com/publon/10.1002/eji.70182.

References

1. G. D. Victora and M. C. Nussenzweig, "Germinal Centers," *Annual Review of Immunology* 40, no. 1 (2022): 413–442, https://doi.org/10.1146/annurev-immunol-120419-022408.

2. A.-K. E. Palm and C. Henry, "Remembrance of Things Past: Long-Term B Cell Memory After Infection and Vaccination," *Frontiers in Immunology* 10 (2019): 1787, https://doi.org/10.3389/fimmu.2019.01787.

3. Z. Liu, Y. Gu, A. Shin, S. Zhang, and F. Ginhoux, "Analysis of Myeloid Cells in Mouse Tissues With Flow Cytometry," *STAR Protocols* 1, no. 1 (2020): 100029, https://doi.org/10.1016/j.xpro.2020.100029.

4. E. Hobeika, M. Dautzenberg, E. Levit-Zerdoun, R. Pelanda, and M. Reth, "Conditional Selection of B Cells in Mice With an Inducible B Cell Development," *Frontiers in Immunology* 9 (2018): 1806, https://doi.org/10.3389/fimmu.2018.01806.

5. M. Verheijen, S. Rane, C. Pearson, and A. J. Yates, "Seddon B. Fate Mapping Quantifies the Dynamics of B Cell Development and Activation Throughout Life," *Cell Reports* 33, no. 7 (2020): 108376, https://doi.org/10.1016/j.celrep.2020.108376.

6. K. T. Mincham, J. D. Young, and D. H. Strickland, "OMIP 076: High-Dimensional Immunophenotyping of Murine T-Cell, B-Cell, and Antibody Secreting Cell Subsets," *Cytometry Part A* 99, no. 9 (2021): 888–892, https://doi.org/10.1002/cyto.a.24474.

7. K. L. Good-Jacobson, E. Song, S. Anderson, A. H. Sharpe, and M. J. Shlomchik, "CD80 Expression on B Cells Regulates Murine T Follicular Helper Development, Germinal Center B Cell Survival, and Plasma Cell Generation," *Journal of Immunology* 188, no. 9 (2012): 4217–4225, https://doi.org/10.4049/jimmunol.1102885.

8. H. Y. Lee, T. Celhar, and A. M. Fairhurst, "Assessing Lupus-Like Disease in Murine Model Systems," *Current Protocols* 1, no. 11 (2021): e272, https://doi.org/10.1002/cpz1.272.

15214141, 2026, 4, Downloaded from https://onlinelibrary.wiley.com/doi/10.1002/eji.70182 by Dagmar Stiek - Deutsches Krebsforschungszentrum (DKFZ) , Wiley Online Library on [09/06/2026]. See the Terms and Conditions (https://onlinelibrary.wiley.com/terms-and-conditions) on Wiley Online Library for rules of use; OA articles are governed by the applicable Creative Commons License

9. N. M. Weisel, S. M. Joachim, S. Smita, et al., "Surface Phenotypes of Naive and Memory B Cells in Mouse and Human Tissues," *Nature Immunology* 23, no. 1 (2021): 135–145, https://doi.org/10.1038/s41590-021-01078-x.

10. R. Riedel, R. Addo, M. Ferreira-Gomes, et al., "Discrete Populations of Isotype-Switched Memory B Lymphocytes Are Maintained in Murine Spleen and Bone Marrow," *Nature Communications* 11, no. 1 (2020): 2570, https://doi.org/10.1038/s41467-020-16464-6.

11. K. Pracht, J. Meinzinger, P. Daum, et al., "A New Staining Protocol for Detection of Murine Antibody-Secreting Plasma Cell Subsets by Flow Cytometry," *European Journal of Immunology* 47, no. 8 (2017): 1389–1392, https://doi.org/10.1002/eji.201747019.

12. X. Liu, J. Yao, Y. Zhao, J. Wang, and H. Qi, "Heterogeneous Plasma Cells and Long-Lived Subsets in Response to Immunization, Autoantigen and Microbiota," *Nature Immunology* 23, no. 11 (2022): 1564–1576, https://doi.org/10.1038/s41590-022-01345-5.

13. G. K. Manakkat Vijay, M. Zhou, and K. Thakkar, "Temporal Dynamics and Genomic Programming of Plasma Cell Fates," *Nature Immunology* 25, no. 6 (2024): 1097–1109, https://doi.org/10.1038/s41590-024-01831-y.

14. M. D. Taylor, M. R. Brewer, A. Nedeljkovic-Kurepa, et al., "CD4 T Follicular Helper Cells Prevent Depletion of Follicular B Cells in Response to Cecal Ligation and Puncture," *Frontiers in Immunology* 11 (2020): 1946, https://doi.org/10.3389/fimmu.2020.01946.

15. F. Alotaibi, M. Vincent, W. P. Min, and J. Koropatnick, "Reduced CD5 on CD8(+) T Cells in Tumors But Not Lymphoid Organs Is Associated With Increased Activation and Effector Function," *Frontiers in Immunology* 11 (2020): 584937, https://doi.org/10.3389/fimmu.2020.584937.

Supporting Information

Additional supporting information can be found online in the Supporting Information section.

Supporting File: eji70182-sup-0001-SuppMat.pdf.

15214141, 2026, 4, Downloaded from https://onlinelibrary.wiley.com/doi/10.1002/eji.70182 by Dagmar Stiek - Deutsches Krebsforschungszentrum (DKFZ) , Wiley Online Library on [09/06/2026]. See the Terms and Conditions (https://onlinelibrary.wiley.com/terms-and-conditions) on Wiley Online Library for rules of use; OA articles are governed by the applicable Creative Commons License